Journal of Alloys and Compounds 650 (2015) 658–663

Contents lists available at ScienceDirect

Journal of Alloys and Compounds

journal homepage: http://www.elsevier.com/locate/jalcom

Temperature dependent current–voltage characteristics of Au/n-type Ge Schottky barrier diodes with graphene interlayer

Zagarzusem Khurelbaatar [a, b], Min-Sung Kang [a], Kyu-Hwan Shim [a], Hyung-Joong Yun [a, c], Jouhan Lee [c], Hyobong Hong [d], Sung-Yong Chang [e], Sung-Nam Lee [f], Chel-Jong Choi [a, *]

[a] School of Semiconductor and Chemical Engineering, Semiconductor Physics Research Center (SPRC), Chonbuk National University, Jeonju 561-756, Republic of Korea
[b] School of Information and Communication Technology, Mongolian University of Science and Technology, Ulaanbaatar 51-29, Mongolia
[c] Division of Material Science, Korea Basic Science Institute, Daejeon 305-806, Republic of Korea
[d] IT Convergence Research Lab., Electronics and Telecommunications Research Institute (ETRI), Daejeon 307-700, Republic of Korea
[e] Power Generation Lab., Korea Electric Power Research Institute (KEPRI), Daejeon 305-380, Republic of Korea
[f] Department of Nano-Optical Engineering, Korea Polytechnic University, Siheung 429-793, Republic of Korea

ARTICLE INFO

Article history:
Received 25 May 2015
Received in revised form
12 July 2015
Accepted 4 August 2015
Available online 8 August 2015

Keywords:
Schottky barrier diode
Graphene
Interlayer
n-type Ge
Gaussian distribution
Barrier inhomogeneity

ABSTRACT

Current–voltage (I–V) characteristics of Au/n-type Ge Schottky barrier diodes (SBDs) with and without graphene interlayer were investigated in the temperature range of 180–340 K. For both devices, the Schottky parameters –such as the barrier height and ideality factor–showed strong temperature dependence, indicating a deviation of the I–V characteristics from what the thermionic emission (TE) mechanism predicts. On the basis of the TE theory along with the assumption that the barrier height takes on a Gaussian distribution, the temperature dependence of the I–V characteristics of the Au/n-type Ge SBDs with and without graphene interlayer was explained in terms of Schottky barrier inhomogeneity. Experimental results reveal the existence of a double Gaussian distribution of barrier height in the Au/n-type Ge SBD, whereas only a single Gaussian distribution of barrier height existed in the Au/graphene/n-type Ge SBD. Furthermore, the degree of barrier inhomogeneity of the Au/graphene/n-type Ge SBD is lower than that of the Au/n-type Ge SBD. The superiority of the Schottky barrier for the Au/graphene/n-type Ge SBD could be associated with the passivation of the Ge surface by the graphene interlayer.

1. Introduction

Graphene has become a valuable material in fundamental science and technology because of its excellent electronic, optical, thermal and mechanical properties [1–4]. The prominent features of graphene have facilitated its application in high-performance devices, including field effect transistors [5], photodetectors [6], light emitting diodes [7], chemical sensors [8] and supercapacitors [9]. For instance, Mayorov et al. [10] reported that high room-temperature mobilities in graphene exceed 100.000 cm^2/V s and over a 1 μm distance ballistic transport. Furthermore, Li et al. [11] demonstrated that graphene can be used not only as a transparent, conductive electrode for light transmission, but also as an active layer for electron/hole separation and hole transport, as well as an antireflection layer in graphene–Si solar cells. Zeng et al. [12] fabricated high-speed photodetectors based on photocurrents generated at the graphene-semiconductor Schottky interface, in which graphene was used as a transparent electrode. Additionally, Schedin et al. [8] demonstrated that graphene is an ideal material for the high-sensitivity gas detection and confirmed that their fabricated sensor had detection limits on the order of one part per billion, the same as that of other existing gas detectors.

Recently, germanium (Ge) has been considered to be a promising channel material for next-generation, high-mobility complementary metal-oxide-semiconductor (CMOS) devices in terms of overcoming the scaling limits of its Si counterpart. A major challenge in the realization of high-performance Ge-based CMOS devices is posed by the effect of strong Fermi-level pinning close to the valence band of Ge [13–16]. This makes it difficult to modulate the barrier heights of metal-Ge junctions via the selection of metals

* Corresponding author.
E-mail address: cjchoi@jbnu.ac.kr (C.-J. Choi).

http://dx.doi.org/10.1016/j.jallcom.2015.08.031
0925-8388/

with different work functions. Some techniques for controlling the barrier height of metal-Ge contacts have been proposed, such as plasma treatment [13], sulfur segregation [14] and the insertion of a thin insulator layer between the metal and Ge [15,16]. Most recently, we investigated the effect of a graphene interlayer on the electrical properties of Au/n-type Ge Schottky barrier diodes (SBDs) using current–voltage (I–V) and capacitance–voltage (C–V) characteristics, and demonstrated that the minimizing the Fermi-level pinning of Ge could be associated with the passivation of Ge surface by graphene [17].

However, despite the prominent features of Au/n-type Ge SBDs with graphene interlayer, detailed information about the Schottky interface –such as temperature dependence of the Schottky barrier parameters–still remains unclear, though this is required for the further enhancement of device performance. As a continuation of our previous work, here we investigated the nature of the Schottky interface of the of Au/graphene/n-type Ge SBD, and directly compare it with that of the Au/n-type Ge SBD in terms of temperature-dependent I–V characteristics. The non-ideal I–V behavior of Au/n-type Ge SBDs with and without graphene interlayer is explained in terms of barrier inhomogeneity assuming that the barrier height takes on a Gaussian distribution. It will be shown that single and double Gaussian distribution of barrier height exist in Au/n-type Ge SBDs with and without graphene interlayer, respectively. It is further shown that, owing to the passivation of the Ge surface by the graphene interlayer, Au/graphene/n-type Ge SBD exhibits more homogeneous Schottky interface than Au/n-type Ge SBD.

2. Experimental details

Large-area, single-layer graphene sheets were grown by chemical vapor deposition (CVD) on high quality polycrystalline copper (Cu) foils (25 μm thick) using a process described elsewhere [18]. A 500 nm-thick PMMA (Micro Chem, 950 PMMA C4) was spin-coated onto the graphene film grown on Cu foil at 3000 rpm for 30 s. Then, the unwanted graphene was removed from the back side of the Cu foils by O_2 plasma process. The Cu was then etched from the PMMA-supported films using a 0.05 mg/L solution of ferric nitride [$Fe(NO_3)_3$], yielding PMMA/graphene sheets. Finally, the PMMA/graphene sheets were washed several times in deionized water and isopropyl alcohol.

Fig. 1 shows schematic diagrams of the fabrication process of the Au/n-type Ge SBD with a graphene interlayer. An n-type (100) Ge wafer with a carrier concentration of 1×10^{16} cm^{-3} was used as the basic substrate. The Ge wafers were initially degreased with organic solvents like acetone and methanol by means of ultrasonic agitation for duration of 5 min in each step to remove contaminants, followed by rinsing in deionized (DI) water and then drying in N_2 flow. The wafers were then etched with a buffered oxide etch (BOE) for 60 s to remove native oxide from the substrate. After the cleaning process, the PMMA/graphene sheet was transferred onto the Ge substrate, followed by the removal of the PMMA film using acetone for 12 h (Fig. 1(a)). The 2D-to-G intensity ratio, calculated from the Raman spectrum taken from graphene transferred onto the Ge substrate, was found to be >2, corresponding to the typical monolayer feature of CVD-grown graphene [19]. Afterward, a circular Au (100 nm) electrode with a diameter of 1 mm was deposited on the graphene through a metal shadow mask by electron-beam evaporator at a pressure of ~3.8×10^{-6} Torr (Fig. 1(b)). At this stage, redundant graphene was removed by reactive-ion etching (RIE) with a power of 30 W, resulting in the formation of a circularly shaped mesa structure, as shown in Fig. 1(c). Finally, in order to form the bottom electrode, a Ga–In eutectic alloy was covered onto the back side surface of Ge substrate (Fig. 1(d)). For a comparison, the intimate Au/n-type Ge SBD without graphene interlayer was fabricated on the n-type Ge substrate under similar process conditions. Namely, after surface cleaning and subsequent removal of native oxide from Ge substrate, the sample was inserted into the deposition chamber of electron-beam evaporator immediately in order to form the circular Au electrode through metal shadow mask. Then, for the formation of the Ohmic contact, metallization using Ga–In eutectic alloy was performed on the back surface of the Ge substrate without RIE process. The I–V measurements of Au/n-type Ge SBDs with and without graphene were performed using a semiconductor parameter analyzer (Agilent 4155C) over the temperature range of 180–340 K in steps of 20 K under dark conditions.

3. Results and discussion

Fig. 2 shows the forward and reverse bias semi-logarithmic I–V characteristics of the Au/n-type Ge SBDs with and without the graphene interlayer over the temperature range of 180–340 K in

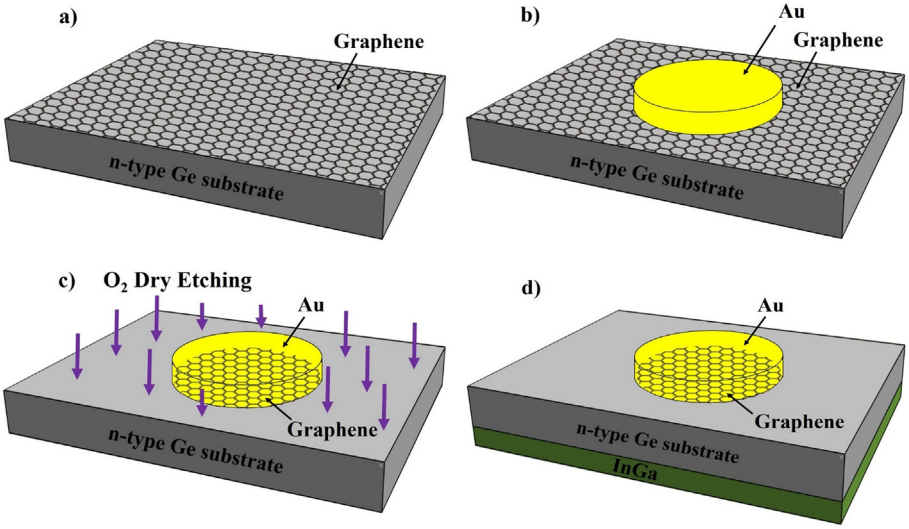

Fig. 1. Schematic diagrams illustrating the procedures for the fabrication of Au/n-type Ge SBD with a graphene interlayer: (a) Graphene transferred onto the Ge substrate, (b) Formation of the circular Au electrode, (c) Removal of redundant graphene using RIE process, and (d) Deposition of Ga–In eutectic alloy as the bottom electrode.

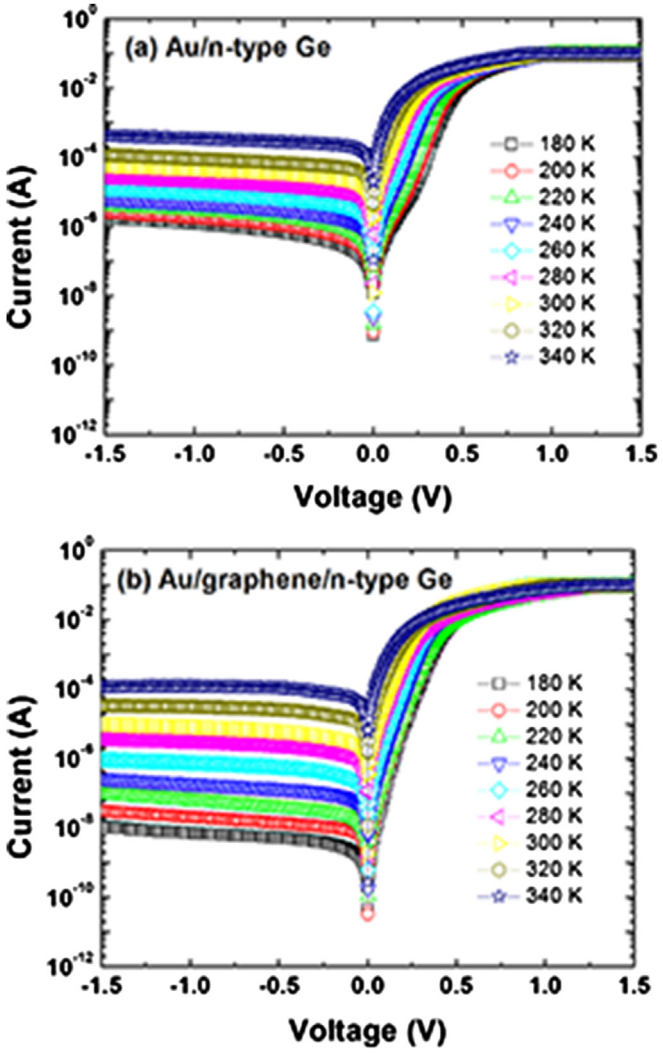

Fig. 2. The forward and reverse bias, semi-logarithmic current–voltage (I–V) characteristics of (a) the Au/n-type Ge SBD and (b) the Au/graphene/n-type Ge SBD over the temperature range of 180–340 K with steps of 20 K.

steps of 20 K. For both devices, the leakage currents increased with increasing temperature. For instance, the reverse leakage currents, measured at −1 V, were found to range from 1.21×10^{-6} A (at 180 K) to 3.46×10^{-4} A (at 340 K) for the Au/n-type Ge SBD, and 7.15×10^{-9} A (at 180 K) to 1.21×10^{-4} A (at 340 K) for the Au/graphene/n-type Ge SBD. It is clear that both SBDs exhibited a typical rectifying behavior with an exponential increase of current in the forward bias and weak voltage dependence of current in reverse bias, implying that the thermionic emission theory can be used for determining the electrical parameters [20,21]. The experimental values of barrier height (Φ_{b0}) and ideality factor (n) were determined from the intercepts and slopes of the forward bias $ln(I)$ versus V plot at each temperature, respectively, and are summarized in Table 1 and Fig. 3. It should be noted that the Φ_{b0} of Au/graphene/n-type Ge SBD was higher than that of Au/n-type Ge SBD. This indicates that the graphene interlayer effectively modified the barrier height by influencing the interfacial potential barrier of the Au/n-type Ge Schottky junction. It can be observed that both devices exhibited the strong temperature dependence of Φ_{b0} and n. For instance, with decreasing temperature, Φ_{b0} and n decreased and increased, respectively. This indicates a deviation from pure TE theory, in which Φ_{b0} and n should remain constant with temperature. Although n deviated from unity for both devices, the Au/graphene/n-type Ge SBD exhibited lower values of n across the entire temperature range, as compared to Au/n-type Ge SBD. Furthermore, the Au/n-type Ge SBD showed wider current spread as a function of temperature than Au/graphene/n-type Ge SBD. Specifically, the current spread of Au/n-type Ge SBD became more widespread in low temperature region that of Au/graphene/n-type Ge SBD, whilst the difference of current spread between both SBDs was insignificant in high temperature region. When considering the dominance of temperature dependence of Φ_{b0} and n in the Au/n-type Ge SBD, wider current spread of Au/n-type Ge junction could be due to the presence of laterally inhomogeneous Schottky barrier with low and high barrier patches. In other words, the barrier inhomogeneity was lower for the Au/graphene/n-type Ge SBD.

The Richardson constant A^{**} can be experimentally determined using a conventional Richardson plot of $ln(I_0/T^2)$ versus $1000/T$ (Fig. 4), which can be obtained as:

$$\ln\left(\frac{I_0}{T^2}\right) = \ln(AA^{**}) - \frac{q\Phi_{bo}}{kT}, \tag{1}$$

According to Eq. (1), $ln(I_0/T^2)$ versus $1000/T$ plot gives a straight line, with the y-intercept yielding the value of A^{**}. The Richardson plot taken from Au/graphene/n-type Ge SBD was linear in the whole measured temperature range. The value of A^{**}, determined from linear fit, was found to be 9.73×10^{-4} A/cm^2 K^2. On the other hand, for the Au/n-type Ge SBD, the $ln(I_0/T^2)$ versus $1000/T$ plot consisted of two linear regions, which appear in low-temperature (180–240 K) and high-temperature (260–340 K) regions. The values of A^{**} calculated from the Au/n-type Ge SBD were found to be 3.64×10^{-7} and 0.24 A/cm^2 K^2 in the temperature ranges of 180–240 K and 260–340 K, respectively. It is worth noting that the values of the Richardson constant experimentally determined from both devices were much lower than the theoretical Richardson constant for n-type Ge (*i.e.*, 140 A/cm^2 K^2). Such a large discrepancy between the experimental and theoretical values of the Richardson constant can be attributed to the fact that the calculation used the temperature-dependent I–V characteristics, which may be affected by the lateral inhomogeneity of the Schottky barrier and potential fluctuations at the Schottky interface [22].

In order to explain the non-ideal I–V behavior of Au/n-type Ge SBDs with and without graphene interlayer, the Gaussian distribution of the Φ_{b0} with a mean barrier height at zero bias $\overline{\Phi}_{bo}$ and a standard deviation σ_o (an analytical potential fluctuation model) was employed, as introduced by Song et al. [23]. The Gaussian distribution of the Φ_{b0} is given by Refs. [24,25]:

$$\Phi_{ap} = \overline{\Phi_{bo}}(T=0) - \frac{q\sigma_0^2}{2kT}, \tag{2}$$

where Φ_{ap} is the apparent barrier height measured experimentally, and σ_0 is the standard deviation of the barrier height distribution. On the basis of Eq. (2), the Φ_{ap} versus $1/2\ kT$ plot (Fig. 5), should produce a straight line yielding $\overline{\Phi}_{bo}$ and σ_0 from the y-axis intercept and slope of the linear fit, respectively. For the Au/graphene/n-type Ge SBD, the values of $\overline{\Phi}_{bo}$ and σ_0 were measured to be 0.87 eV and 0.107 eV, respectively. In spite of that, for the Au/n-type Ge SBD, the plot of Φ_{ap} versus $1/2\ kT$ exhibited two linear regions, implying the presence of two Gaussian distributions of Φ_{b0} in Schottky junction. From the corresponding calculations using the intercepts and slopes of these straight lines, values of $\overline{\Phi}_{bo}$ and σ_0 were found to be 0.81 and 0.111 eV, respectively, in the temperatures ranging of 180–240 K; as well as 0.92 and 0.125 eV, respectively, in the temperatures ranging of 260–340 K. The temperature dependence of σ_0

Table 1
Temperature-dependent values of various parameters determined from *I–V* characteristics of Au/n-type Ge SBDs with and without graphene interlayer.

Temperature (K)	I_o (A)		n		Φ_{bo}(eV)	
	Without graphene	With graphene	Without graphene	With graphene	Without graphene	With graphene
180	6.54×10^{-8}	9.44×10^{-10}	2.25	1.28	0.41	0.50
200	1.10×10^{-7}	4.79×10^{-9}	2.06	1.25	0.45	0.52
220	1.88×10^{-7}	9.12×10^{-9}	1.84	1.19	0.49	0.56
240	3.68×10^{-7}	2.99×10^{-8}	1.69	1.15	0.51	0.59
260	8.96×10^{-7}	1.08×10^{-7}	1.39	1.13	0.53	0.60
280	2.63×10^{-6}	5.25×10^{-7}	1.22	1.08	0.59	0.63
300	8.87×10^{-6}	1.71×10^{-6}	1.10	1.06	0.61	0.64
320	2.84×10^{-5}	8.97×10^{-6}	1.07	1.03	0.63	0.66
340	1.42×10^{-4}	3.95×10^{-5}	1.02	1.02	0.65	0.67

is usually small enough to be negligible. However, for Au/n-type Ge SBDs with and without graphene interlayer, the values of σ_0 are not small compared with the values to $\overline{\Phi}_{bo}$. This implies the existence of Schottky barrier inhomogeneity, which affects the temperature-dependent *I–V* characteristics of both devices. Furthermore, σ_0 is a measure of the barrier homogeneity. Lower values of σ_0 correspond to more homogeneous Φ_{b0}. It should be noted that the σ_0 extracted from the Au/graphene/n-type Ge SBD was relatively lower than that from Au/n-type Ge SBD over the entire temperature range.

As described earlier, for Au/n-type Ge SBDs with and without graphene interlayer, the Richardson constant extracted from a conventional Richardson plot (Fig. 4) was much lower than the theoretical value of the Richardson constant, owing to barrier inhomogeneity. Taking into account the barrier inhomogeneity, a more reliable value of the Richardson constant can be calculated by employing modified Richardson plot (Fig. 6), which was obtained by following expression [26]:

$$\ln\left(\frac{I_0}{T^2}\right) - \left(\frac{q^2\sigma_0^2}{2k^2T^2}\right) = \ln(AA^{**}) - \frac{q\overline{\Phi}_{bo}}{kT}, \quad (3)$$

Fig. 6 shows the modified Richardson plot of $ln(I_0/T^2)$-$(q\sigma_0)^2/2(kT)^2$ versus $1000/T$ for Au/n-type Ge SBDs with and without a graphene interlayer. A fit to the modified Richardson plot should be a straight line, from which the slope and y-axis intercept yield the mean Schottky barrier height $\overline{\Phi}_{bo}$ and the modified Richardson constant A^{**} for a given diode area, respectively. From this plot of the Au/graphene/n-type Ge SBD, the mean Schottky barrier height and the modified Richardson constant were determined to be 0.87 eV and 128 AK^{-2} cm^{-2}, respectively. These values were in good agreement with the mean Schottky barrier height (0.87 eV) extracted from the plot of Φ_{ap} versus $1/2\ kT$ (Fig. 6) and the theoretical value of Richardson constant for n-type Ge (140 AK^{-2} cm^{-2}). On the other hand, for Au/n-type Ge SBDs without a graphene interlayer, with a double Gaussian distribution of barrier height, the mean Schottky barrier height and the modified Richardson constant were found to be 0.76 eV and 7.9 AK^{-2} cm^{-2}, respectively, in the low-temperature region (180–240 K); along with 0.93 eV and 532.8 AK^{-2} cm^{-2}, respectively, in the high-temperature region (260–340 K). In the low temperature region, the modified Richardson constant was much smaller than the theoretical value. This could be attributed to the greater inhomogeneity at the Schottky interface [27]. In other word, a significant barrier inhomogeneity prevailing at the interface in low temperature region led to the reduction of the intimate effective area (which represents only a small fraction of the geometric area) interested by the current flow, which could be responsible for the incongruity between experimental and theoretical Richardson constant [28]. Whereas, at higher temperature, owing to the variation of barrier height with temperature, the modified Richardson constant was larger than the theoretical value [29,30].

Based on the modified Richardson plot (Fig. 6) combined with the Φ_{ap} versus $1/2\ kT$ plot (Fig. 5), it can be concluded that Au/graphene/n-type Ge SBD had more homogenous Schottky barrier

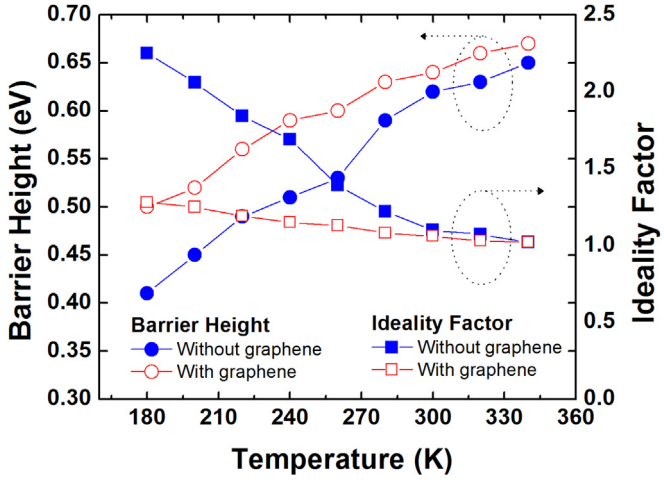

Fig. 3. Temperature dependence of the ideality factor and barrier height taken from Au/n-type Ge SBDs with and without the graphene interlayer measured at temperatures in the range of 180–340 K.

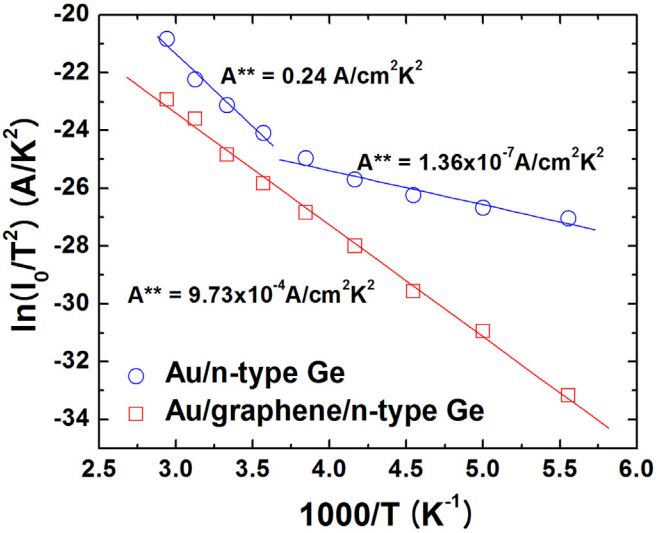

Fig. 4. Richardson plots of $ln(I_0/T^2)$ versus $1000/T$ for the Au/n-type Ge SBDs with and without the graphene interlayer.

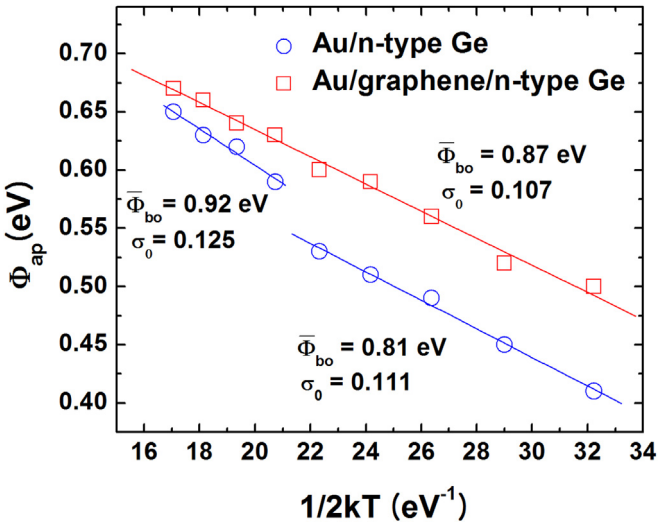

Fig. 5. Plots of Φ_{ap} as a function of *1/2kT*for Au/n-type Ge SBDs with and without the graphene interlayer.

interface than Au/n-type Ge SBD. Generally, barrier inhomogeneity is unavoidable as they can exist even in carefully prepared samples. The barrier inhomogeneity may occur as a result of the poor interface quality, which, in turn, depends on several factors such as the surface and bulk defect density distribution, the inhomogeneities in the interfacial thin layer stoichiometry, compositional changes at the near surface region, non-uniformity of the interfacial charge distribution, and interfacial layer thickness [26,31]. In a present work, Au/n-type Ge SBDs with and without graphene interlayer were fabricated using similar process condition. Moreover, the graphene transfer and RIE processes were added in the fabrication of Au/n-type Ge SBD with graphene interlayer, implying that additional process-induced defects might cause the barrier inhomogeneity of Au/graphene/n-type Ge SBD. Nevertheless, our experimental results revealed that the barrier of Au/graphene/n-type Ge SBD was more homogeneous than that of Au/n-type Ge SBD. Such an improvement of Schottky nature of Au/graphene/n-type Ge SBD could be associated with the reduction of interface state density (N_{ss}) in Schottky interface caused by the surface passivation of Ge by graphene interlayer. Namely, the

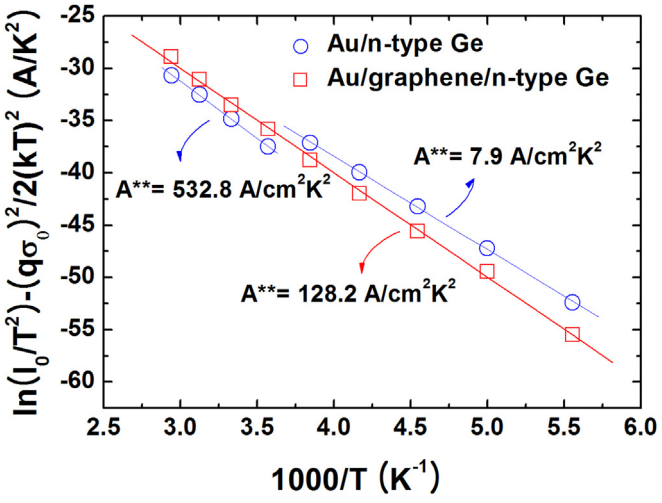

Fig. 6. Modified Richardson plots of $ln(I_0/T^2)-(q\sigma_0)^2/2(kT)^2(A/K^2)$ versus *1000/T* for the Au/n-type Ge SBDs with and without the graphene interlayer.

surface states of Ge surface responsible for the Fermi level pinning of Ge could be a main cause of barrier inhomogeneity prevailing in Au/n-type Ge SBD. In fact, the plots of N_{ss} calculated from forward bias I–V data by taking the voltage-dependent ideality factor with the effective barrier height proposed by Card and Rhoderick [32] as a function of temperature (not shown here) revealed that the Au/graphene/n-type Ge SBD showed lower N_{ss} than the Au/n-type Ge SBD at all the temperatures. Furthermore, the N_{ss} is sufficiently high to strong affect band alignment, then this would lead to an increase in barrier heights from its original value [33]. In other word, the effective barrier height extracted by considering Gaussian spatial distribution of barrier height associated with N_{ss} might be higher than barrier height calculated by conventional forward I–V characteristics based on pure thermionic emission model. In addition, as compared with the Au/graphene/n-type Ge SBD, a relatively larger variation of the barrier heights with temperature was observed in Au/n-type Ge SBD. This inhomogeneous Schottky barrier nature of Au/n-type Ge SBD resulted in overestimating the barrier height. Thus, the combined effect of higher N_{ss} and stronger temperature dependency of barrier height in Au/n-type SBD caused that the effective barrier height of Au/n-type SBD was higher than that of Au/graphene/n-type SBD especially in high temperature region as shown in Figs. 5 and 6.

4. Conclusions

The Schottky barrier interface of the Au/graphene/n-type Ge SBD was investigated using temperature dependent *I–V* characteristics, and was directly compared with that of the Au/n-type Ge SBD. Owing to barrier inhomogeneity, the Au/n-type Ge SBDs with and without graphene interlayer showed the anomalous temperature dependence of Schottky barrier parameters; more specifically, with increasing temperature, the n decreased and Φ_{b0} increased. The plot of Φ_{ap} versus *1/2 kT* revealed that the degree of barrier inhomogeneity of the Au/graphene/n-type Ge SBD with the single Gaussian distribution of barrier heights was relatively lower than that of Au/n-type Ge SBD with the double Gaussian distribution of barrier heights. This was also confirmed by employing modified Richardson plot, in which the modified Richardson constant of Au/graphene/n-type Ge SBD was close to the theoretical value for n-type Ge; by way of contrast, there was a relatively large discrepancy between the experimentally determined modified Richardson constant and its theoretical value for n-type Ge in Au/n-type Ge SBD. A direct comparison of temperature-dependent *I–V* characteristics between Au/n-type Ge SBDs with and without graphene interlayer showed that the introduction of the graphene interlayer between Au and n-type Ge led to suppression of barrier inhomogeneity in Schottky interface, which could be associated with the reduction of native defects in Ge surface caused by the passivation of the Ge surface by the graphene interlayer.

Acknowledgments

This research was supported by a grant from the R&D Program (Grant no. 10045216) for Industrial Core Technology funded by the Ministry of Trade, Industry and Energy (MOTIE), Republic of Korea, and by Converging Research Center Program (2014M3C1A8048834) through the Ministry of Science, ICT & Future Planning, Republic of Korea. It was also financially supported by Basic Science Research Program (NRF-2015R1A6A1A04020421) through the National Research Foundation of Korea (NRF) funded by the Ministry of Education, Republic of Korea.

References

[1] K.S. Novoselov, A.K. Geim, S.V. Morozov, D. Jiang, Y. Zhang, S.V. Dubonos, I.V. Grigorieva, A.A. Firsov, Electric field in atomically thin carbon films, Science 306 (2004) 666–669.

[2] R.R. Nair, P. Blake, A.N. Grigorenko, K.S. Novoselov, T.J. Booth, T. Stauber, N.M.R. Peres, A.K. Geim, Fine structure constant defines visual transparency of graphene, Science 320 (2008) 1308.

[3] A.A. Balandin, S. Ghosh, W. Bao, I. Calizo, D. Teweldebrhan, F. Miao, C.N. Lau, Superior thermal conductivity of single-layer graphene, Nano Lett. 8 (2008) 902–907.

[4] I.W. Frank, D.M. Tanenbaum, A.M. Van Der Zande, P.L. McEuen, Mechanical properties of suspended graphene sheets, J. Vac. Sci. Technol. 25 (2007) 2558–2561.

[5] Y. An, A. Behnam, E. Pop, A. Ural, Metal-semiconductor-metal photodetectors based on graphene/p-type silicon Schottky junction, Appl. Phys. Lett. 102 (2013), 013110–1-013110-5.

[6] J.T. Wang, J.M. Ball, E.M. Barea, A. Abate, J.A. Alexander Webber, J. Huang, M. Saliba, I. Mora-Sero, J. Bisquert, H.J. Snaith, R.J. Nicholas, Low-temperature processed electron collection layers of graphene/TiO_2 nanocomposites in thin film perovskite solar cells, Nano Lett. 14 (2014) 724–730.

[7] T.H. Seo, B.K. Kim, G. Shin, C. Lee, M.J. Kim, H. Kim, E.K. Suh, Graphene-silver nanowire hybrid structure as a transparent and current spreading electrode in ultraviolet light emitting diodes, Appl. Phys. Lett. 103 (2013), 051105–1-051105-5.

[8] F. Schedin, A.K. Gein, S.V. Morozov, E.W. Hill, P. Blake, M.I. Katsnelson, K.S. Novoselov, Detection of individual gas molecules adsorbed on graphene, Nat. Mat. 9 (2007) 652–655.

[9] J. Li, X. Cheng, J. Sun, C. Brand, A. Shashurin, M. Reeves, M. Keidar, Paper-based ultracapacitors with carbon nanotubes-graphene composites, J. Appl. Phys. 115 (2014), 164301–1-164301-5.

[10] A.S. Mayorov, R.V. Gorbachev, S.V. Morozov, L. Britnell, R. Jalil, L.A. Ponomarenko, P. Blake, K.S. Novoselov, K. Watanabe, T. Taniguchi, A.K. Geim, Micrometer-scale ballistic transport in encapsulated graphene at room temperature, Nano Lett. 11 (2011) 2396–2399.

[11] X. Li, H. Zhu, K. Wang, A. Cao, J. Wei, C. Li, Y. Jia, Z. Li, X. Li, D. Wu, Graphene-on-silicon Schottky junction solar cells, Adv. Mater. 22 (2010) 2743–2748.

[12] L.H. Zeng, M.Z. Wang, H. Hu, B. Nie, Y.Q. Yu, C.Y. Wu, L. Wang, J.G. Hu, C. Xie, F.X. Liang, L.B. Luo, Monolayer graphene/germanium Schottky junction as high-performance self-driven infrared light photodetector, ACS Appl. Mater. Interfaces 5 (2013) 9362–9366.

[13] J.R. Wu, Y.H. Wu, C.Y. Hou, M.L. Wu, C.C. Lin, L.L. Chen, Impact of fluorine treatment on Fermi level depinning for metal/germanium Schottky junction, Appl. Phys. Lett. 99 (2011), 253504–1-253504-3.

[14] K. Ikeda, Y. Yamashita, N. Sugiyama, N. Taoka, S. Takagi, Modulation of NiGe/Ge Schottky barrier height by sulfur segregation during Ni germanidation, Appl. Phys. Lett. 88 (2006), 152115–1-152115-3.

[15] V. Janardhanam, H.J. Yun, J. Lee, V. Rajagopal Reddy, H. Hong, K.S. Ahn, C.J. Choi, Depinning of the Fermi level at the Ge Schottky interface through Se treatment, Scr. Mater. 69 (2013) 809–811.

[16] A. Dimoulas, P. Tsipas, A. Sotiropoulos, E.K. Evangelou, Fermi-level pinning and charge neutrality level in germanium, Appl. Phys. Lett. 89 (2006), 252110–1-252110-2.

[17] Z. Khurelbaatar, Y.H. Kil, H.J. Yun, K.H. Shim, J.T. Nam, K.S. Kim, S.K. Lee, C.J. Choi, Modification of Schottky barrier properties of Au/n-type Ge Schottky barrier diode using monolayer graphene interlayer, J. Alloy. Compd. 614 (2014) 323–329.

[18] H. Kim, Y. Kim, T.Y. Kim, A.R. Jang, H.Y. Jeong, S.H. Han, D.H. Yoon, H.S. Shin, D.J. Bae, K.S. Kim, W.S. Yang, Enhanced optical response of hybridized VO_2/graphene films, Nanoscale 5 (2013) 2632–2636.

[19] A.C. Ferrari, J.C. Meyer, V. Scardaci, C. Casiraghi, M. Lazzeri, F. Mauri, S. Piscanec, D. Jiang, K.S. Novoselov, S. Roth, A.K. Geim, Raman spectrum of graphene and graphene layers, Phys. Rev. Lett. 97 (2006), 187401–1-187401-4.

[20] E.H. Rhoderick, R.H. Williams, Metal-semiconductor Contacts, second ed., Clarendon, Oxford, 1988.

[21] S.M. Sze, Physics of Semiconductor Devices, second ed., Wiley, New York, 1981.

[22] Z.J. Horvath, Comment on "analysis of I–V measurements on $CrSi_2$/Si Schottky structure in a wide temperature range", Solid-State Electron 39 (1996) 176–178.

[23] Y.P. Song, R.L. Van Meirhaeghe, W.H. Laflere, F. Cardon, On the difference in apparent barrier height as obtained from capacitance–voltage and current–voltage–temperature measurements on Al/p-InP Schottky barriers, Solid-State Electron 29 (1986) 633–638.

[24] R.F. Schmitsdorf, T.U. Kampen, W. Mönch, Correlation between barrier height and interface structure of AgSi (111) Schottky diodes, Surf. Sci. 324 (1995) 249–256.

[25] S. Chand, J. Kumar, Effects of barrier height distribution on the behavior of a Schottky diode, J. Appl. Phys. 82 (1997) 5005–5010.

[26] I. Jyothi, Min-Woo Seo, V. Janardhanam, Kyu-Hwan Shim, Young-Boo Lee, Kwang-Soon Ahn, Chel-Jong Choi, Temperature-dependent current–voltage characteristics of Er-silicide Schottky contacts to strained Si-on-insulator, J. Alloy. Compd. 556 (2013) 252–258.

[27] A. Chawanda, W. Mtangi, F.D. Auret, J. Nel, C. Nyamhere, M. Diale, Current-voltage temperature characteristics of Au/n-Ge (100) Schottky diodes, Phys. B 407 (2012) 1574–1577.

[28] V. Saxena, J.N. Su, A.J. Steckl, High-voltage Ni-and Pt-SiC Schottky diodes utilizing metal field plate termination, IEEE Trans. Electron Dev. 46 (1999) 456–464.

[29] J.M. Borrego, R.J. Gutmann, S. Ashok, Richardson constant of Al-and Au-GaAs Schottky barrier diodes, Appl. Phys. Lett. 30 (1977) 169–172.

[30] A.K. Srivastava, B.M. Arora, S. Guha, Measurement of Richardson constant of GaAs Schottky barriers, Solid-State Electron 24 (1981) 185–191.

[31] A. Ashok Kumar, V. Rajagopal Reddy, V. Janardhanam, Hyun-Deok Yang, Hyung-Joong Yun, Chel-Jong Choi, Electrical properties of Pt/n-type Ge Schottky contact with PEDOT: PSS interlayer, J. Alloy. Compd. 549 (2013) 18–21.

[32] H.C. Card, E.H. Rhoderick, Studies of tunnel MOS diodes I. Interface effects in silicon Schottky diodes, J. Phys. D. Appl. Phys. 4 (1971) 1589–1601.

[33] M.O. Aboelfotoh, Electrical characteristics of WSi(100) Schottky barrier junctions, J. Appl. Phys. 66 (1989) 262–272.